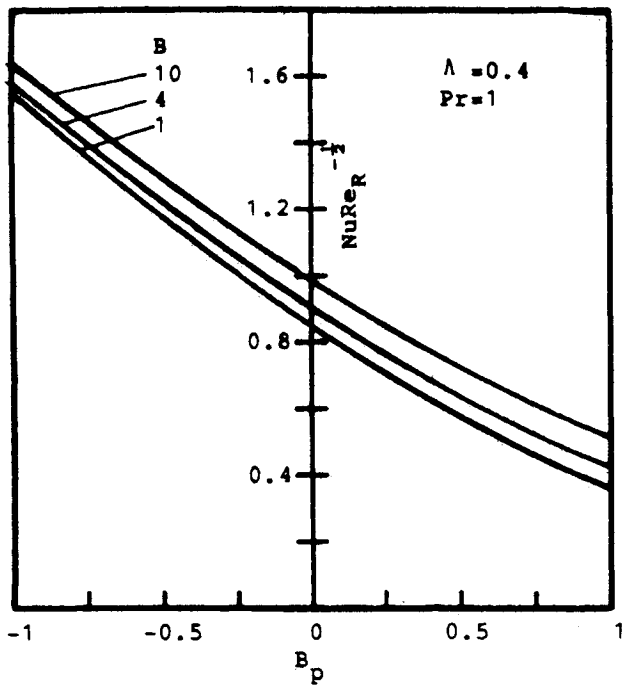

Fig. 3 Local Nusselt number as a function of the mass-transfer parameter B_p for various rotation parameters B of constant heat-flux surface.

Results and Discussion

We use a two-point finite difference method to solve the system (4-7). This is a very efficient numerical method developed by Cebeci and Bradshaw.[4]

Figure 1 shows that for a given value of rotation parameter B $(4/9(R\Omega/u_\infty)^2\Lambda)$, the wall shear decreases monotonically with B_p as the suction intensity decreases from -1 to 0 and the injection intensity increases from 0 to 1. The ordering of the curves with rotation parameter B is governed by the angular velocity of the rotating body. An increase in the value of the rotation parameter yields an increase in the value of the local friction coefficient when the other conditions are fixed.

Figures 2 and 3 show that for a given value of rotation parameter B, the local surface heat-transfer rate of isothermal surface or constant-heat-flux surface, like that of the wall shear, decreases monotonically as the suction intensity decreases and as the injection intensity increases. The ordering of the curve is the same as in Fig. 1. The higher rates of the surface heat transfer associated with larger values of rotation parameter B are due to the increase in the axial velocity that results in enhancing the convective heat-transfer rate between the body and the fluid.

For comparison of our numerical results for wall shear and Nusselt number without blowing and suction, Lee et al.'s[3] Merk-type series formula and Hoskin's[2] Blasius-type solutions were used. The results are included in Tables 1 and 2 and show excellent agreement with our result.

References

[1]Siekmann, J., "The Calculation of the Thermal Laminar Boundary Layer on a Rotating Sphere," *Zeitschrift für Angewandte Mathemathik und Physik*, Vol. 13, 1962, p. 468.

[2]Hoskin, N. E., "The Laminar Boundary Layer on a Rotating Sphere," *50 Jahre Grenzschichtforschung*, edited by H. Gortler and W. Tollmien, 1955, pp. 127-131.

[3]Lee, M. H., Jeng, D. R., and Dewitt, K. J., "Laminar Boundary Layer Transfer over Rotating Bodies in Forced Flow," *Journal of Heat Transfer*, Vol. 100, 1978, pp. 496-502.

[4]Cebeci, T. and Bradshaw, P., "Momentum Transfer in Boundary Layers," Hemisphere Publishing Corp., Washington, D.C., 1977, pp. 213-234.

Aluminum Combustion at 40 Atmospheres Using a Reflected Shock Wave

J.F. Driscoll,* J.A. Nicholls,† V. Patel,‡
B.K. Shahidi,‡ and T.C. Liu§
University of Michigan, Ann Arbor, Michigan

Introduction

IT has been found that an ideal way to study the reactions between aluminum and the gases N_2, H_2, Cl_2, and O_2 at elevated pressures up to 40 atm and temperatures up to 5150 K is to use a reflected shock wave within a shock tube. A technique was developed in which a heated, thin aluminum sheet is placed on the end wall of a single pulsed shock tube filled with the desired gaseous reactants. After a shock wave reflects off the end wall, elevated pressures and temperatures up to 40 atm and 5000 K were achieved. Pressure is constant during the run time of 10 ms which is more than adequate to study the fast reactions that occur. A diffusion flame is formed between the aluminum sheet and the hot reactant gases. Emission spectroscopy was used to identify some important intermediate species in the flame. The time histories of the species concentrations obtained in this way can yield useful chemical kinetics data.

In the past, extensive studies of aluminum-based rocket propellant fuels have conducted in order to develop ways to control the amount and size of Al_2O_3 particles in rocket exhausts. Aluminum particles can increase plume visibility, radiative heating of the nozzle, and two-phase flow losses. Controllable laboratory experiments that have been used to study aluminum combustion are the fast flow reactor,[1,2] the burning of aluminum ribbons,[3,4] and the use of incident shock waves in a shock tube.[5,6] However, the first two techniques have been limited to pressures of a few atmospheres or less. Reactions that occur at elevated pressures in rocket motors may differ from those that occur at 1 atm. The use of incident shock waves expose the aluminum to supersonic velocities that may not be be desired. The use of a reflected shock, as described in this Note, provides a stagnant gas environment at much higher pressures and temperatures than even incident shock waves can provide.

Experimental Method

An aluminum sample (2 cm × 2 cm) having thickness that varied from 0.01 to 0.1 cm was mounted on the end wall of a single-pulse shock tube.[7] The 4.7 m long driver section has an i.d. of 7.4 cm, and the 6.7 m long driven section has inner dimensions of 7.4 cm × 4.8 cm. The driven gas was either pure O_2 or the mixture $0.1\ N_2 + 0.4\ H_2 + 0.1\ Cl_2 + 0.4\ O_2$, which has the same elemental composition as ammonium perchlorate. For a driven gas pressure of 0.026 atm and a helium driver gas pressure of 102 atm, the incident shock Mach number was 10.5, and the temperature and pressure behind the reflected shock were 5150 K and 40 atm,

Presented as Paper 84-1201 at the AIAA/SAE/ASME 20th Joint Propulsion Conference, Cincinnati, OH, June 11-13, 1985; revision received Aug. 14, 1985.

*Associate Professor, Aerospace Engineering. Member AIAA.
†Professor, Aerospace Engineering. Fellow AIAA.
‡Research Assistant.
§Visiting Scientist, Institute of Aeronautics and Astronautics, Beijing, China.

Table 1 List of species identified in the emission spectrum of the Al + 0.1 N_2 + 0.4 H_2 + 0.1 Cl_2 + 0.4 O_2 reaction at 40 atm pressure, 5150 K

Species	Wavelength, Å
Al	3944, 3961.
Al+	5861
AlO	4648, 4842, 5079, 5337
H	4340, 4861, 6563
O	5350
O+	4880
N	4103, 5666, 5679
AlH	4241,4259

respectively. Conditions behind the reflected shock were determined from the NASA Gordon-McBride computer code. Pressure was measured to be constant during the effective test time of 10 ms, which ended when the expansion wave that had reflected off the driver tube end wall reached the aluminum sample.[7]

Results

The ignition temperature of aluminum in pure oxygen at elevated pressures was measured and compared to the known ignition temperature at 1 atm. Data obtained for pressure up to 7 atm showed that the aluminum ignition temperature was 2390 K. This is only slightly higher than the ignition temperature at 1 atm, which has been found to be 2303 K by Macek.[4] The value of 2303 K corresponds to the melting point the Al_2O_3 oxide that forms a protective covering over the sample. Small particles of aluminum were observed to be emitted from the sample surface, probably due to local boiling of the molten metal. These particles were observed to ignite at temperatures as low as 2000 K, probably because they had no oxide covering.

The species observed in the photographs of the emission spectra are listed in Table 1. The spectral bands identified in the present Note could be used in future work with more sophisticated diagnostics, including laser Raman and laser fluorescence techniques. One advantage of the shock tube technique is that spectral bands can be positively identified. For example, when spectral bands overlap, the hydrogen can be easily removed from the gas mixture, and all bands resulting from hydrogenated species will disappear. In addition to species listed in Table 1, other bands thought to belong to OH, AlOH, and $AlCl_2$ were observed but not positively identified. Spectral bands belonging to the important species AlO_2 and Al_2O_2 were unfortunately not strong enough to be identified in the visible spectrum even at elevated temperatures up to 5000 K.

Some of the more important species that can take part in the reaction are shown in Fig. 1. The values in Fig. 1 represent the equilibrum composition at 40 atm, calculated using the NASA Gordon-McBride computer code. While equilibrium concentrations are of interest, of more interest is the information about the rate of species formation that is made possible by the use of a shock tube.

Figure 2 shows the measured time history of the light emitted by AlO at 4846 Å in the diffusion flame near the shock tube end wall. For comparison, the time history of the continuum at 4500 Å is also plotted. The continuum is generally believed to be due to condensed Al_2O_3 droplets.[8] The rate at which AlO and Al_2O_3 are produced can be inferred from the slopes of the curves in Fig. 2; however, further work is needed to relate the AlO and Al_2O_3 concentratons to the measured light intensities. The rate of formation of AlO and Al_2O_3 is clearly limited by the diffusion of Al and O_2 and not by the chemical kinetics.

The Al_2O_3 particles that represent products of combustion were examined under an electron microscope. For Al reacting with pure O_2, the Al_2O_3 particles were perfect spheres of diameter 0.1 to 0.6 μm. However, the presence of HCl in the products caused the Al_2O_3 to agglomerate into 20 μm long strands. It is believed that the condensed HCl acts as nucleation site that agglomerate the particles. The end gas was analyzed using infared gas absorption analysis; the amount of HCl and H_2O detected was in agreement with equilibrium estimates, but the level of NO and NO_2 was three orders of magnitude greater than equilibrium estimates. The slow NO reactions, therefore, must be kinetically limited as in hydrocarbon flames.

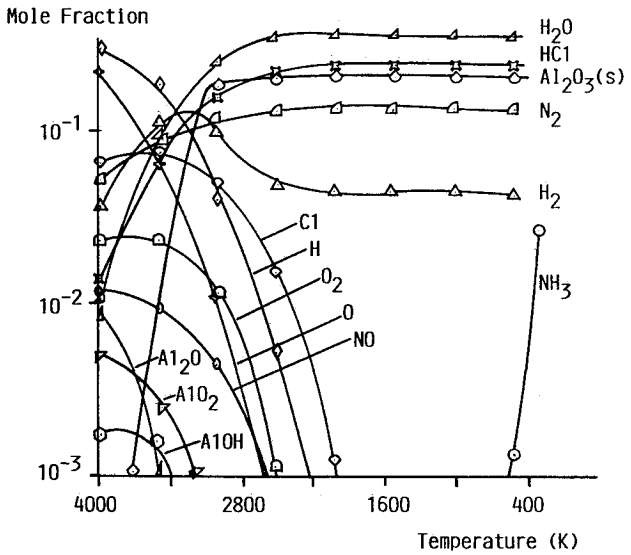

Fig. 1 Predicted equilibrium concentration in the Al + 0.1 N_2 + 0.4 H_2 + 0.1 Cl_2 + O_2; reaction using NASA Gordon-McBride program.

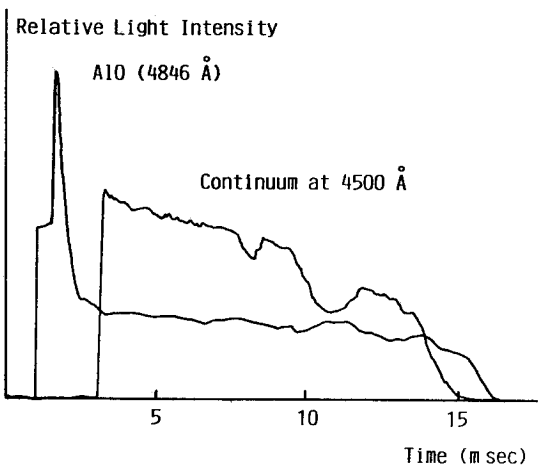

Fig. 2 Time history of light emitted from AlO and from continuum at 4500 Å in aluminum-oxygen reaction at 40 atm pressure, 5150 K.

Acknowledgments

This research was supported by the U.S. Air Force Rocket Propulsion Laboratory, Edwards, California, under contract F04611-79-C-0030.

References

[1]Mann, D. M., "Particulate Formulation in Al-O_2 Flames," 15th JANNAF Combustion Meeting, CPIA Pub. 297, Chemical Prop. Inf. Agency, Newport, RI, Feb. 1979.

[2]Fontijn, A., Felder, W., and Houghton, J., "HTFFR Kinetic Studies. Temperature Dependence of Al/O_2 Kinetics," Sixteenth Symposium (International) on Combustion, The Combustion Institute, Pittsburgh, PA, 1977, p. 871.

[3]Brustowski, T. and Glassman, I., "Spectroscopic Investigation of Metal Combustion," *Heterogeneous Combustion, Progress in Astronautics and Aeronautics*, Vol. 15, 1964, AIAA, New York, p. 41.
[4]Friedman, R. and Macek, A., "Combustion Studies of Single Aluminum Particles," Ninth Symposium (International) on Combustion, 1963, p.703.
[5]Kashiwagi, T., Kotia, G., and Summerfield, M., "Flame Spread of a Solid Fuel in a Hot Oxidizing Gas Stream," *Combustion and Flame*, Vol. 24, May 1975, p. 357.
[6]Fox, T., TeVelde, J., and Nicholls, A., "Shock Wave Ignition of Metal Particles," *Proceedings of the 1976 Heat Transfer and Fluid Mechanics Conference*, edited by A. McKillop, Stanford Univ. Press, 1976.
[7]Lifshitz, A. and Bauer, S.H., "Studies with a Single Pulse Shock Tube," *Journal of Chemical Physics*, Vol. 38, No. 9, 1963, p. 2056.
[8]Rautenberg, T. H. and Johnson, P. D., "Light Production in the Aluminum-Oxygen Reaction," *Journal of the Optical Society America*, Vol. 50, No. 6, 1960, p.602.

Spiral Vortices and Liquid Breakup

L. K. Isaacson*
University of Utah, Salt Lake City, Utah

Introduction

INTERNAL cavity flows occur in many engineering environments, including the internal flow in solid-propellant rocket motors. Liquids occur in the metalized solid-propellant rocket motor environment in the form of molten aluminum or aluminum oxide droplets.[1] This Note reports on the observation of axially directed spiral vortices in an internal cavity flow and the breakup of a liquid droplet placed in the initiation point of a vortex. With the occurrence of axially directed spiral vortices from wall shear layers[2] and from separated free shear layers as indicated in this Note, a dynamic process is identified that could provide a key mechanism for breaking liquid aluminum and aluminum oxide droplets and agglomerates from propellant surfaces in aluminized solid-propellant rocket motors.

Experimental Facilities and Results

This study was carried out in the Subsonic Turbulent Flow Facility in the Department of Mechanical and Industrial Engineering at the University of Utah. This facility and the internal flow cavity employed in the study are described in Ref. 3.

The flow facility has a test section 2.44 m in length and a cross section 177.8 mm on a side. The first 0.61 m of the top surface of the test section is covered with a medium coarse sandpaper to promote transition of the boundary layer to a turbulent flow state. A schematic of the internal flow cavity is shown in Fig. 1, with the location of the free shear layers indicated in the diagram. Velocity profiles were obtained with an X-configuration, constant-temperature, hot-film anemometer system with linearized output signals. Mean velocity values were obtained as the average of 50 samples at each vertical location in the flow region. The axial velocity profile shown in Fig. 2 was obtained with a traversing mechanism driven with a computer-controlled stepper motor with 1,000 vertical steps in increments of 0.08 mm, for a total distance of 80 mm across the center of the flow region. This profile was obtained at an axial distance of 2 mm downstream of the edge of the forward restrictors. The Reynolds shear stress profile shown in Fig. 3 was obtained with a Honeywell model 9410 correlator for this same axial station.

The Reynolds shear stress was obtained with a boundary-layer type of probe with X-configuration sensors. The probe was inserted from the bottom wall of the cavity with the sensors intersecting the free shear layer velocity gradient from below. Probe-induced flow oscillations should be minimized with this procedure.[4]

The Reynolds shear stress profile indicates several significant aspects of the flow in the upper and lower free shear layers. Note that the upstream turbulent nature of the incoming boundary layer has a dramatic effect on the Reynolds shear stress in the upper free shear layer, as previously indicated by Hussain and Clark,[5] with a large component of velocity fluctuations carried into the free shear layer from the upstream turbulent boundary layer along the top wall of the test section.

The Reynolds shear stress profile through the lower free shear layer indicates the presence of four counterrotating, axially directed vortices. The possible existence of the axial vortex structures was noted initially by the discovery of high-frequency, high-intensity velocity fluctuations ("turbulent bursts") at a distance of approximately 2 mm downstream and 2 mm above the edge of the lower forward restrictor. These bursts were not observed forward of a station 1 mm downstream and 2 mm above the edge of the lower restrictor. These bursts are similar to the bursts observed by Lindgren,[6] as reported by Joseph,[7] and are also similar to the bursts observed in wall shear layers by Blackwelder and Eckelmann[2] and Maslowe.[8]

In these experiments, we are primarily interested in identifying the interaction of counterrotating pairs of vortices and liquid droplets. Water is injected into the flow stream with a 0.5 mm needle with the liquid injection point placed in the mainstream flow and the liquid allowed to run down the needle until it is held in place at the critical layer in the shear layer. The droplet is held in place by the vertical velocity component induced by the lower pair of counterrotating vortices. The droplet, which forms on the downstream side of the needle, is observed to oscillate and then to separate into multiple droplets, with several droplets swept from the supporting needle surface. A portion of the orginal droplet remains on the surface of the needle. Figure 4 shows several larger droplets with unstable ligaments of fluid between them. These ligaments break up into smaller droplets. Downstream of the injection point, the larger droplets swept from the supporting needle deform into a parachute-like shape prior to breakup due to aerodynamic effects. Note that the injection needle was placed at the entrance to the flow cavity and that the flow is from right to left in the photograph of Fig. 4.

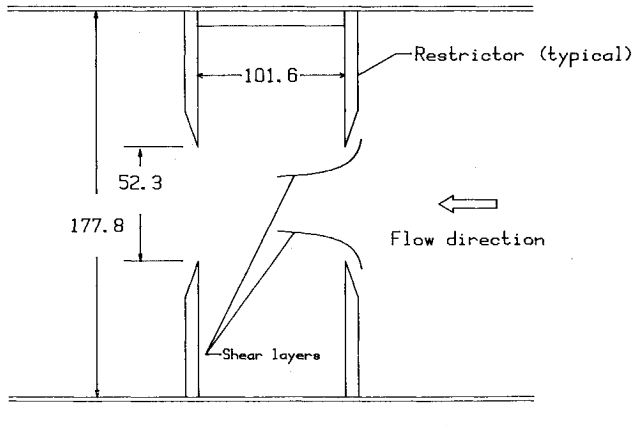

Note: All dimensions are in millimeters

Fig. 1 Schematic diagram of the internal flow cavity showing the curved shear layers in the forward region of the cavity.

Received Jan. 24, 1985; revision received Sept. 4, 1985.

*Professor of Mechanical Engineering. Associate Fellow AIAA.